General Disclaimer

One or more of the Following Statements may affect this Document

- This document has been reproduced from the best copy furnished by the organizational source. It is being released in the interest of making available as much information as possible.

- This document may contain data, which exceeds the sheet parameters. It was furnished in this condition by the organizational source and is the best copy available.

- This document may contain tone-on-tone or color graphs, charts and/or pictures, which have been reproduced in black and white.

- This document is paginated as submitted by the original source.

- Portions of this document are not fully legible due to the historical nature of some of the material. However, it is the best reproduction available from the original submission.

NASA TECHNICAL MEMORANDUM

NASA TM X-71909

NASA TM X-71909

MODAL STRUCTURE INFERRED FROM STATIC FAR-FIELD NOISE DIRECTIVITY

by Arthur V. Saule
Lewis Research Center
Cleveland, Ohio 44135

TECHNICAL PAPER to be presented at the Third Aero-Acoustics Conference, sponsored by the American Institute of Aeronautics and Astronautics
Palo Alto, California, July 20-23, 1976

MODAL STRUCTURE INFERRED FROM STATIC FAR-FIELD NOISE DIRECTIVITY

by Arthur V. Saule
National Aeronautics and Space Administration
Lewis Research Center
Cleveland, Ohio 44135

ABSTRACT

Turbofan noise directivity calculated for two directivity models (equal modal amplitude and equal modal power or energy) was compared with experimental, blade passing frequency data from two fans at 60 and 90 percent speeds. Experimental data indicated similar directivity patterns which were well represented by a single average data curve. Calculated points using the equal amplitude model showed over-prediction near the fan axis and near the 90°-position. Calculated points using the equal power model showed a very good match with the average data lending support to theory of equipartition of modal power from a random source such as the interaction of the rotor with inlet flow distortion. The equal modal power model also gave good agreement with individual data points.

E-8704

INTRODUCTION

The modal structure of the internal noise field and its in-duct spatial variation are important to at least two phenomena related to fan noise. First, the modal structure helps to determine the external acoustic radiation pattern or directivity of the sound from a fan stage. Second, the modal structure strongly influences the design of the acoustic treatment for fan inlet ducts (e.g., ref. 1). It is, then, of interest to know the modal structure of the sound produced by a fan stage.

Direct determination of modal structure is a difficult task requiring sophisticated measurement and analysis techniques that, at present, are not performed routinely on fan stages. An alternative approach involves the matching of measured and predicted far-field directivity characteristics. This problem is generally complicated by the multiplicity of possible sound modes of unknown amplitude, as in the case of noise produced by the interaction of the rotor and inlet flow distortion. Current evidence suggests that, especially during ground static testing, disturbances in the inlet flow are the major source of the tone noise (e.g., ref. 2). The modal analysis, therefore, is not performed routinely on far-field directivity data either.

The need to know the in-duct modal structure, as well as the availability of a wealth of far-field directivity data, provided the motivation for the work presented here. The objective of this work was to explore some of the available directivity data relative to the known directivity properties of the possible propagating modes to see if any valid conclusions about the in-duct modal structure could be drawn.

In the approach discussed here, the multiplicity of sound modes was dealt with directly by assuming that all propagating or cut-on modes contribute to the resultant directivity level. The total number of contributing modes was found by applying the mode cut-off criteria to the mode eigenvalues. The second aspect of the problem concerning unknown modal amplitudes required a search for the best combination of elementary directivity patterns in order to reconstruct the actual resultant directivity level. Results of two theoretical directivity models are discussed and presented here: equal-amplitude and equal-energy.

The equal-amplitude directivity model assumes that the duct modal amplitudes are equal. The modal directivity as used in this paper pertains to the far-field elementary directivity patterns due to a single duct mode. The elementary theoretical directivity patterns were calculated using an acoustic radiation model similar to that developed by Morse before the advent of turbofan engines for a flexible piston in an infinite flanged duct without flow[3]. Its application to ducted fan sources producing single spinning modes was investigated by Tyler and Sofrin[4]. Lansing, et al. (ref. 5) considered unflanged duct inlets; their flanged duct radiation model was adopted for this presentation. The assumption of equal-amplitude propagating modes has been used, for example, by Ko for predicting the total sound attenuation of acoustically lined ducts[6].

The modal amplitudes of the equal-energy model are not constant, but vary from mode to mode, while modal acoustic power remains constant for all the modes. This model was developed using Lansing's, et al. (ref. 5) closed-form solution for the radiated modal power from an infinite, nonreflecting duct without flow. Dyer[7] has shown that equal energy distribution among all the duct modes may result from a spatially random source excitation in the fan inlet. Pickett's theoretical analysis[8] has also shown similar results that, at a given frequency, the acoustic energy of the noise caused by unsteady nonuniform inflow to fans with relatively low subsonic tip speeds may be carried in more or less equal quantities by all the propagating duct modes. Yurkovich[9] has recently used equal-energy in the propagating duct modes to compute the total noise attenuation in acoustically-lined ducts and reported good agreement with measured data.

Far-field directivity data obtained at NASA Lewis Research Center from two different full-scale high bypass ratio fans, B and QF-3 (refs. 10 and 11, respectively) were used for comparison with computed directivity patterns. Although these fans were designed for fundamental tone cutoff, both produced high-intensity noise at blade passing frequency, presumably because of inlet flow distortion. Altogether, four sets of blade passing frequency noise data were considered for two operating speeds, 60 to 90 percent. Each data set has seven data points corresponding to the azimuthal locations of seven fixed far-field microphones.

SYMBOLS

A amplitude

B number of rotor blades

c speed of sound, m/sec

D directivity

f	frequency, Hz
J_m	Bessel function of first kind of order m
J'_m	derivative of Bessel function with respect to entire argument
j	distortion index
K	coefficient of modal acoustic pressure, N/m^2
$\bar{k}$	frequency parameter, $2\pi f r_d/c$
k'	eigenvalue
m	circumferential mode order
n	harmonic index
$P(R, \phi)$	far-field point at R and ϕ
p	acoustic far-field pressure, N/m^2
R	far-field radius, m
r_d	duct outer radius, m
r_0	radial coordinate of duct inlet face, m
$S(r_0, \theta_0)$	simple point source at duct inlet face at r_0 and θ_0
x	axial coordinate of acoustic radiator, m
ΔSPL	relative sound pressure level, dB
ϕ	azimuth angle, degrees
μ	radial mode order
θ_0	angular coordinate of duct inlet face, degrees

Subscripts:

m, μ	mode (m, μ)

Superscripts:

(EA)	equal-amplitude
(EE)	equal-energy

MODEL OF ACOUSTICAL RADIATOR

Figure 1 shows a sketch of the geometry for the analytical model of acoustical radiation considered. It consists of a semi-infinite circular duct with uniform cross section. The duct inlet face lies flush with an infinite flange. It is assumed that both, the duct and flange have acoustically hard walls.

The internal noise field within the circular duct is assumed to be made up of sound pressure waves traveling forward in the direction of the duct inlet. The sound pressure waves are assumed to result from a number of spinning modes. Mode reflection, diffraction, and coupling at the duct inlet are neglected. The acoustic medium is assumed to be ideal, stationary air.

For the acoustic radiation model shown in figure 1, the sound radiates into free unbounded space from a distributed source over the duct inlet face. This source consists of a distribution of simple point sources or monopoles of differing strength arising from air particles vibrating with a nonuniform velocity. The sound pressure advances from the source as spherical wavelets. Since the infinite flange prevents radiation toward the rear, the external noise field in front of the flanged duct assumes a shape of an axisymmetric half-sphere centered at the center of the duct inlet face.

A segment of external noise field is shown in figure 1 by a semicircular dashed curve. The far-field acoustic pressure of a single mode, (say, at $P(R, \phi)$ where R and ϕ are azimuthal radius and angle, respectively) is an integral representing the combined contributions from all simple point sources, say, at $S(r_0, \theta_0)$, where r_0 and θ_0 are the coordinates of the duct inlet face.

DIRECTIVITY MODELS

In general, the variables which describe the integrated far-field acoustic pressure due to a single mode can be conveniently arranged as a product of three terms, such as:

$$p_{m,\mu} = (K)(A_{m,\mu})(D_{m,\mu}) \tag{1}$$

where m and μ are the circumferential lobe number and radial mode number of the duct modes under consideration. It is assumed that each term (K, $A_{m,\mu}$, and $D_{m,\mu}$) contains variables with certain common characteristics.

The coefficient K consists of variables which remain constant for a given fan, its operating and testing conditions, and the particular directivity model used. It is independent of modal orders m and μ, and azimuthal angle. Therefore, the coefficient K is used here as a normalizing or weighting factor so that far-field modal acoustic pressures, having the same K, can be compared on the basis of $A_{m,\mu}$ and $D_{m,\mu}$ only. The acoustic power amplitude has been absorbed into K to cause the theory and the data to agree in magnitude. Only relative directivities are considered here, not absolute magnitudes of noise.

The relative duct mode amplitudes are given by $A_{m,\mu}$ since, as just stated, absolute magnitudes have been shifted into the coefficient K. Finally, $D_{m,\mu}$ contains the relative directivity information for each duct mode which shows how the far-field pressure varies with the azimuthal angle ϕ. Thus, for constant K, the total radiated far-field acoustic pressure at any given azimuthal location can be expressed as follows:

$$p = K \sum_{m} \sum_{\mu} (A_{m,\mu}\, D_{m,\mu}) \tag{2}$$

Two directivity models are considered herein: equal-amplitude and equal-energy.

Equal-Amplitude Model

Since for a given fan, with its operating conditions, testing parameters, and source frequency, the amplitudes of all the participating modes in this directivity model are equal, the modal amplitude can be taken, for all practical purposes, to be equal to unity, that is

$$A^{(EA)}_{m,\mu} = 1 \tag{3}$$

For the equal-amplitude directivity model, equation (1) takes on the following form:

$$p^{(EA)}_{m,\mu} = K^{(EA)}\, D^{(EA)}_{m,\mu} \tag{4}$$

In equation (4), it is assumed that all the far-field modal acoustic pressures, which are equally

weighted, can be compared on the basis of the directivity function $D_{m,\mu}^{(EA)}$ only. Here, it is tacitly understood that only far-field modal acoustic pressures with the same coefficient $K^{(EA)}$ can be compared.

A directivity function for this situation has been proposed by Lansing, et al. (ref. 5):

$$D_{m,\mu}^{(EA)} = \frac{J_m(k'_{m,\mu})(\bar{k}\sin\phi)J'_m(\bar{k}\sin\phi)}{(k'_{m,\mu})^2 - (\bar{k}\sin\phi)^2} \qquad (5)$$

Equation (5) describes the directivity of far-field acoustic pressure and was developed for an infinite flanged duct without flow and neglecting reflections.

Lansing, et al. (ref. 5) found that the approximate formula agreed very well with a more exact equation for an unflanged duct at high and low frequencies except at near right angles to the axis and behind the duct inlet. Experimental comparisons indicate that equation (5) gives fairly good agreement with fixed microphone data (e.g., ref. 4). Cumpsty[12] has also reported good results with this approximate equation used to identify lobes from polar shapes of a single microphone traverse.

In equation (5), the argument $k'_{m,\mu}$ of Bessel function $J_m(k'_{m,\mu})$ (eigenvalue of mode (m,μ)) is determined from the solution of the following equation:

$$J'_m(k'_{m,\mu}) = \frac{dJ_m(k'_{m,\mu})}{dk'_{m,\mu}} = 0 \qquad (6)$$

where, for inlet flow distortion noise, the order m is related to frequency harmonic index n, fan rotor blade number B, and distortion harmonic index j (e.g., ref. 8):

$$m = nB \pm j \qquad (7)$$

Since the distortion harmonic index j depends on the extent of the expansion of distortion components into Fourier series, the order m, as seen from equation (7), and consequently, the number of cut-on modes participating in the external radiation field may become quite large, depending on the cut-off conditions:

$$\bar{k} \geq k'_{m,\mu} \qquad (8)$$

where

$$\bar{k} = \frac{2\pi f r_d}{c} \qquad (9)$$

is a frequency parameter involving the source frequency f, duct radius r_d, and speed of sound c.

Equal-Energy Model

For the equal-energy directivity model, an expression is sought which will relate mode amplitude to modal power. Modal power may be obtained by integrating the time average of the far-field sound intensity over the surface area of a hemisphere. Since sound intensity can be expressed as a function of the sound pressure, and since the acoustic power of the equal-energy directivity model is, by definition, equal for all the participating modes, the required relations for mode amplitude can be expressed as follows:

$$(KA_{m,\mu}) = \left[\int_0^{\pi} \left|D_{m,\mu}\right|^2 \sin\phi \, d\phi\right]^{-0.5} \qquad (10)$$

where K, $A_{m,\mu}$, and $D_{m,\mu}$ are used in the same sense as in equation (1). The integral has been evaluated in reference 5 for the power transmitted down an infinite nonreflecting duct without flow. The integrated expression together with other variables and constants are rearranged to conform with the term characteristics as in equation (1) to yield for the equal-energy directivity model the following expression:

$$p_{m,\mu}^{(EE)} = K^{(EE)} A_{m,\mu}^{(EE)} D_{m,\mu}^{(EA)} \qquad (11)$$

where the directivity function $D_{m,\mu}$ as given by equation (5) is used. The modal amplitude for the equal-energy model, $A_{m,\mu}$ is expressed as follows:

$$A_{m,\mu}^{(EE)} = \left\{\frac{\bar{k}\sqrt{\bar{k}^2 - (k'_{m,\mu})^2}}{J_m^2(k'_{m,\mu})\left[1 - \left(\frac{m}{k'_{m,\mu}}\right)^2\right]}\right\}^{0.5} \qquad (12)$$

It is seen from equation (12) that the amplitude varies from mode to mode. It is, therefore, used in combination with the modal directivity function to give

$$D_{m,\mu}^{(EE)} = A_{m,\mu}^{(EE)} D_{m,\mu}^{(EA)} \qquad (13)$$

Substituting equation (13) into equation (11) yields:

$$p_{m,\mu}^{(EE)} = K^{(EE)} D_{m,\mu}^{(EE)} \qquad (14)$$

Since, by definition, the modal pressure coefficient $K^{(EE)}$ for a given fan, operating conditions, testing parameters, and frequency remains constant, there is an equal weighting for all the participating modes.

The nature of the equal-energy modal amplitude $A_{m,\mu}^{(EE)}$ given by equation (12) can be inferred from figure 2 where the amplitude level in decibels is plotted against the circumferential mode order m (from 1 to 37) with radial mode order μ (from 0 to 11) as a parameter for an arbitrarily chosen value of the frequency parameter $\bar{k} = 40$. Altogether, 205 cut-on modes are represented in this figure. It is seen from figure 2 that all the constant μ-order curves start with modes $(1, \mu)$ (axisymmetric modes $(m = 0)$ are excluded from this example), and that for relatively large μ-orders, such as, 9, 10, and 11, the maximum levels are at $m = 1$. The levels of other curves (having μ-orders from 0 to 8) reach their maxima at some order m and then decrease to their minima which, for all 12 curves shown on the figure, is the last cut-on mode for that curve. The largest maximum level of all curves appears for the zero μ-order curve at m-order equal to 28. The maximum level of other curves, having a relatively low μ-order,

also occurs at relatively large m-orders although less than 28. Note in equation (5) that the directivity function peaks when the denominator equals zero and thus $\sin \phi = k'_{m,\mu}/\bar{k}$. Thus, the directivity function peaks at higher angles for larger $k'_{m,\mu}$ for a given value of k. Hence, the behavior of the parametric curves (fig. 2) implies that equal-energy amplitude $A^{(EE)}_{m,\mu}$ puts more emphasis on the modes which peak at the middle angles of the inlet quadrant arc than on the modes which peak near the fan axis or near the 90°-position.

OVERALL DATA CHARACTERISTICS

Far-field directivity data of the blade passing frequency tonal noise obtained from two full-scale high bypass ratio fans, B and QF-3, at 60 and 90 percent design speeds are used for comparison with computed directivity patterns. Altogether, four different data sets are considered herein. Representative design and acoustic properties of fans B and QF-3 are listed in table I, indicating considerable differences between the two fans in the number of rotor blades, stator vanes, total pressure ratios, and source frequencies or wave numbers.

Spectral Characteristics

Fans B and QF-3 belong to a group of NASA-Lewis full-scale high bypass ratio fans which were designed for cut-off of the fundamental tones. Despite this built-in cut-off, these fans, when tested in the same acoustic outdoor static test facility, produced relatively high-intensity noise at blade passing frequency as illustrated in figure 3. The figure shows a narrow-band (4 Hz bandwidth) spectral distribution of the sound pressure level of fan B at 40° azimuthal angle for a sample run at 90 percent design speed. The figure is dominated by this prominent discrete tone spike at blade passing frequency. Similar outstanding discrete frequency tones were also displayed by fan QF-3 narrowband spectra.

Another distinctive feature of the spectrum shown is a concentration of narrow-band random noise at the base of the discrete tone resulting in a considerable noise skirt or base broadening. Similar spectral characteristics have also been observed by Pickett[8] who interpreted these spectral features as a sign of inlet flow distortion noise.

Sound Pressure Level

The data used herein for comparison with calculated directivity patterns are so-called referred sound pressure levels obtained from narrow-band spectra similar to that shown in figure 3 but with atmospheric attenuation removed. The method used for the tone resolution is described in reference 10. The measurements from seven inlet quadrant microphones were used. The microphones were placed 10 degrees apart and 6.7 meters above the ground plane on a 30.5-meter radius arc, the origin of which was located near the exhaust plane of the bypass nozzle. Since the azimuthal angles of the theoretical model considered herein were measured from the duct inlet face (fig. 1), the angle of the experimental data were adjusted to account for this difference. The adjusted sound pressure levels of the blade passing frequency tones of fans B and QF-3 are plotted in figures 4(a) and 4(b) against the azimuthal angle for 60 and 90 percent speeds, respectively. A notable feature of figure 4, despite the indicated differences between the two fans in table I, is the similar azimuthal behavior of the data, especially for the 90 percent speed case.

Directivity

In order to obtain a better directivity measure of the sound pressure level, each data set shown in figure 4 was normalized with respect to its maximum level. The normalized data then were averaged into a single value for each fan. Figure 5 shows a comparison of the normalized average data of the two fans. The indicated points of each fan are the arithmetic averages of two normalized data points at any given angular location. It is seen that they can be well represented by the following empirical equation:

$$\Delta SPL = -8.12 + 0.63\,\phi - 0.0045\,\phi^2 \qquad (15)$$

with azimuth angle ϕ in degrees. This indicated similarity in the measured far-field directivity data points to a possible common noise source, such as, the interaction of the rotor with an unsteady nonuniform inflow consisting of atmospheric turbulence eddies (e.g., ref. 8) or installation caused flow distortion (e.g., ref. 2).

MODAL ANALYSIS OF DIRECTIVITY DATA

Figure 5 shows that the empirical curve of average normalized directivity level rises at first with a relatively slow rate to a broad maximum and then descends toward the 90°-position with a rate which is almost twice that of ascent. Similar azimuthal characteristics have also been noted by several other independent observers (e.g., refs. 13 and 14). These characteristics have been attributed to the data obtained during static tests of fans and compressors, resulting from the interaction of inlet flow distortion and rotor blades.

In theoretical aeroacoustics, it is generally understood (e.g., ref. 15) that since internal modal structure determines the external acoustic radiation pattern or directivity, then the inverse problem of determining unknown in-duct modal field from known far-field directivity should also be, at least in principle, possible to solve. This approach to modal analysis is usually based on the premise that for any given combination of in-duct modes there exists a unique far-field directivity pattern. The results of figure 5, however, seem to contradict this assumption because the different fans and operating conditions represented in the figure will likely produce different modes and amplitudes that should significantly vary among the cases considered (table I). Nevertheless, the figure shows that the resultant directivities of these modes apparently differ but little from each other.

This contradiction, however, may be resolved realizing that as the frequency increases, more and more cut-on modes are propagating through a duct cross-sectional area. As a result, the spatial (radial and angular) variations of the duct acoustic pressure, on the average, are expected to become smaller and smaller for a random noise source (e.g., ref. 7). Consequently, similar in-duct modal structures may result in and may account for similar far-field directivity patterns as shown in figure 5.

The following work then was undertaken to

further explore some of the directivity data relative to the known, calculated elementary directivity properties of possible propagating duct modes to see if, when using this approach, any conclusions could be drawn. Since apparently there is no simple way of finding the right combination of possible propagating duct modes which may participate in the external radiation field it was assumed that all the cut-on modes (eq. (8)) are propagating and participating. The resultant directivity was calculated by using equation (4) for equal-amplitude and equation (14) for equal-energy directivity models. A comparison of theoretical and average experimental directivity for the equal-amplitude directivity model is shown in figure 6(a) for fans B and QF-3, each at 60 and 90 percent design speeds. It is seen that, in general, the calculated directivity levels near the fan axis and near the 90°-position consistently indicate higher levels than the average data curve (eq. (15)). Moreover, it appears that the calculated points near the 90°-position overpredict the data more and more as the total number of participating cut-on modes increases (see table I where more modes at 90 percent than at 60 percent speeds are shown).

The nature of equal-energy modal amplitude given by equation (12) was illustrated in figure 2 where the particular behavior of the parametric curves implies that equal-energy amplitudes put more weight on the modes which peak at the middle angles of the inlet quadrant arc than on the modes which peak near the fan axis or near the 90°-position. This effect is even more evident in figure 6(b) where the calculated resultant relative directivity levels for the equal-energy directivity model are compared with the average experimental curve. The figure shows a very good match between the empirical curve and the calculated points regardless of fan and speed or number of participating cut-on modes.

It is also of interest to make a similar comparison between points calculated by using the equal-energy directivity model and individual experimental data points (fig. 4) to see if any relatively large differences will show up that might be missed during the previous comparison with average data because the latter have a tendency to smooth out differences. Figure 7(a) shows a comparison of the theoretical directivity level for the equal-energy model with individual data points of fan B at 60 and 90 percent speeds. Figure 7(b) shows a similar comparison for fan QF-3. The figures indicate a good agreement between data and calculated levels for both fans, especially at 90 percent speed. At 60 percent speed the agreement is reasonably good, indicating relatively small deviations from the data points.

CONCLUDING REMARKS

The work discussed in this report was undertaken to explore some of the available directivity data relative to the known directivity properties of the possible propagating modes to see if any conclusions about the in-duct modal structure could be drawn. The total number of propagating duct modes which are participating in the external noise field was found by applying the mode cut-off criteria. The theoretical directivity patterns were obtained for two modal energy distribution models. The first model assumed equal duct mode amplitudes. The second model assumed that the inlet duct modes carry equal acoustic power or energy into the far-field. The two radiation models were checked against four arbitrarily selected data sets representing blade passing frequency noise from two different fans (B and QF-3) tested at two different speeds (60 and 90 percent).

Inspection of the data indicated a distinctive concentration of narrow-band random noise at the base of the discrete BPF tone in the form of a considerable noise skirt or base broadening, characteristic of inlet flow distortion-rotor interaction noise. The data, when normalized and averaged, showed similar directivity patterns, regardless of the fan and operating speed. Comparison of theoretical directivities obtained from the two directivity models with averaged data curves indicated a very good match with the equal-energy directivity model, while the calculated points from the equal-amplitude directivity model showed some overpredicting of the data near the fan axis and near the 90°-position. Comparison with individual data also showed a good agreement, with relatively small deviations at 60 percent speed, when the equal-energy directivity model was used.

The apparent good agreement between calculated and experimental data using the equal-energy directivity model may lend further support to the proposition that equipartition of modal energy may be characteristic of random noise sources. The similar directivity patterns that occurred regardless of speed and fan may be considered as additional evidence of inlet flow distortion noise, and consequently of the possible existence of similar in-duct modal structure. The results are encouraging and further studies of directivity data are warranted. Inasmuch as direct determination of modal structure is still in the development stage, the wealth of far-field directivity test data, practically unused to date for intensive modal analysis, may provide additional motivation for such an effort.

Modal information is vital in the design of inlet duct suppressors. However, for turbofan engines, the ultimate goal is noise reduction under flight conditions. Inlet flow distortion may not be the dominant factor in the noise generation, and equal duct modal energy may no longer apply in flight. Nevertheless, the techniques, based on modal theory, may still be applicable to flight directivity data. Finally, the static far-field directivity data may be of some use also for flight situations to obtain an idea about modal structure in flight if periodic signals can be recovered from higher harmonic static data.

REFERENCES

1. Rice, E. J., "Acoustic Liner Optimum Impedance for Spinning Modes with Mode Cutoff Ratio as the Design Criterion," paper to be presented at the AIAA Third Aero-Acoustic Conference, July 1976, Palo Alto, California.

2. Povinelli, F. P.; Dittmar, J. H.; and Woodward, R. P., "Effect of Installation Caused Flow Distortion on Noise From a Fan Designed for Turbofan Engines," NASA TN D-7076, Nov. 1972.

3. Morse, Philip M., Vibration and Sound, McGraw-Hill Book Co., New York, 1948.

4. Tyler, J. M. and Sofrin, T. G., "Axial Flow Compressor Noise Studies," SAE Transactions, Vol. 70, 1962, pp. 309-332.

5. Lansing, D. L., Drischler, J. A., and Pusey, C. G., "Radiation of Sound from an Unflanged Circular Duct with Flow," paper presented at the 79th Meeting of the Acoustical Society of America, Atlantic City, New Jersey, April 21-24, 1970.

6. Ko, Sung-Hwan, "Theoretical Prediction of Sound Attenuation in Acoustically Lined Annular Ducts in the Presence of Uniform Flow and Shear Flow," Journal of the Acoustical Society of America, Vol. 54, June 1973, pp. 1592-1606.

7. Dyer, I., "Measurements of Noise Sources in Ducts." Journal of the Acoustical Society of America, Vol. 30, Sept. 1958, pp. 833-841.

8. Pickett, G. F., "Effects of Nonuniform Inflow on Fan Noise," paper presented at the Spring Meeting of Acoustical Society of America, New York City, April 23-26, 1974.

9. Yurkovich, R., "Attenuation of Acoustic Modes in Circular and Annular Ducts in the Presence of Sheared Flow," AIAA Paper 75-131, Pasadena, Calif., 1975.

10. Saule, A. V., "Some Observations About the Components of Transonic Fan Noise from Narrow-band Spectral Analysis," NASA TN D-7788, Oct. 1974.

11. Dittmar, J. H., and Groeneweg, J. F., "Effect of Treated Length on the Performance of Full-Scale Turbofan Inlet Noise Suppressors," NASA TN D-7826, Dec. 1974.

12. Cumpsty, N. A., "Tone Noise from Rotor/Stator Interactions in High Speed Fans," Journal of Sound and Vibration, Vol. 24, Oct. 1972, pp. 393-409.

13. Burdsall, E. A., and Urban, R. H., "Fan-Compressor Noise; Prediction, Research, and Reduction Studies," 1971, Pratt & Whitney Aircraft (FAA-RD-71-73), East Hartford, Conn.

14. Heidmann, M. F., "Interim Prediction Method for Fan and Compressor Source Noise," NASA TM X-71763, June 1975.

15. Morse, P. M. and Ingard, U. K., Theoretical Acoustics, McGraw-Hill Book Co., New York, 1968.

TABLE I. - DESIGN AND ACOUSTIC CHARACTERISTICS

OF FANS B AND QF-3

A. Design Characteristics

Description	Fan B	Fan QF-3
Number of rotor blades, B	26	53
Number of stator vanes, V	60	112
Rotor inlet tip radius, r_d, meters	0.93	0.91
Total pressure ratio	1.5	1.4

B. Acoustic Characteristics

Description	Fan B		Fan QF-3	
	Percent design speed			
	60	90	60	90
Rotor tip Mach number	0.63	0.94	0.60	0.89
Source frequency, f, hertz	925	1390	1890	2830
Source wavenumber, $\bar{k}$	16.3	24.4	31.6	47.3
Total number of cut-on modes at BPF[a]	34	78	127	284

[a]Blade passage frequency

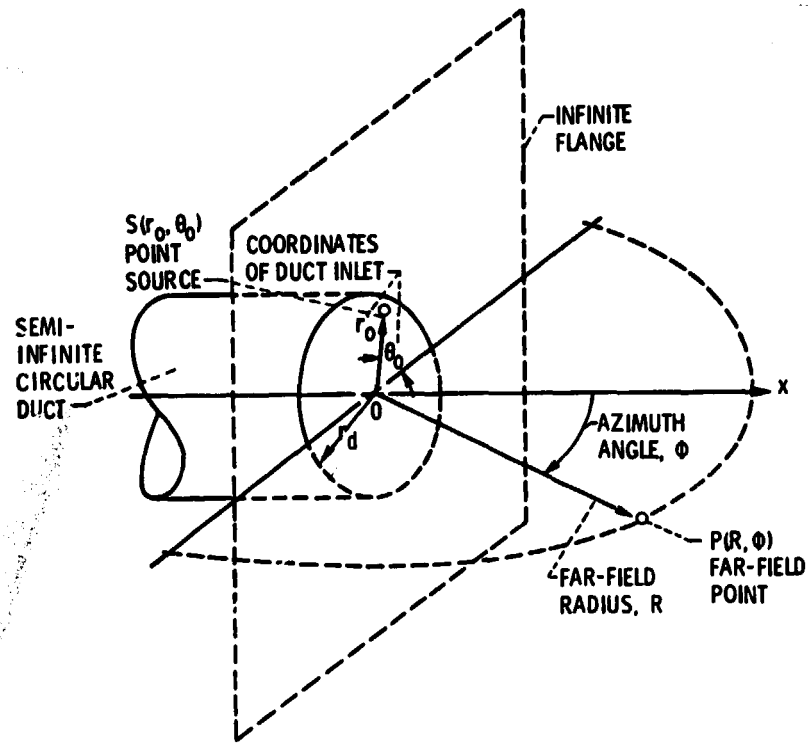

Figure 1. - Sketch of acoustic radiation model.

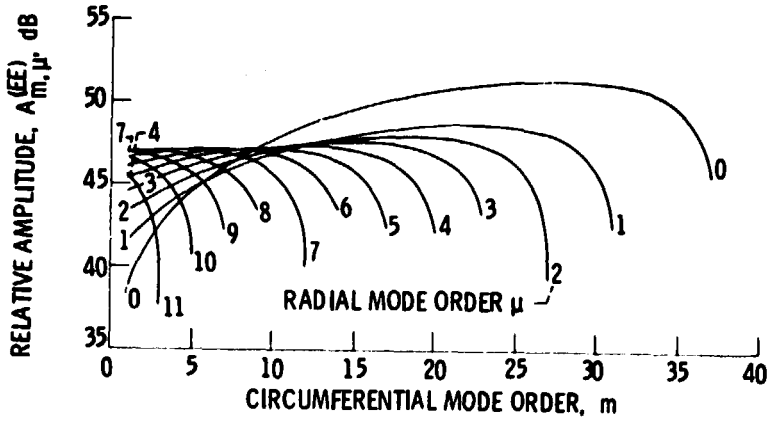

Figure 2. - Variation of mode amplitudes of equal energy directivity model with mode orders (K = 40).

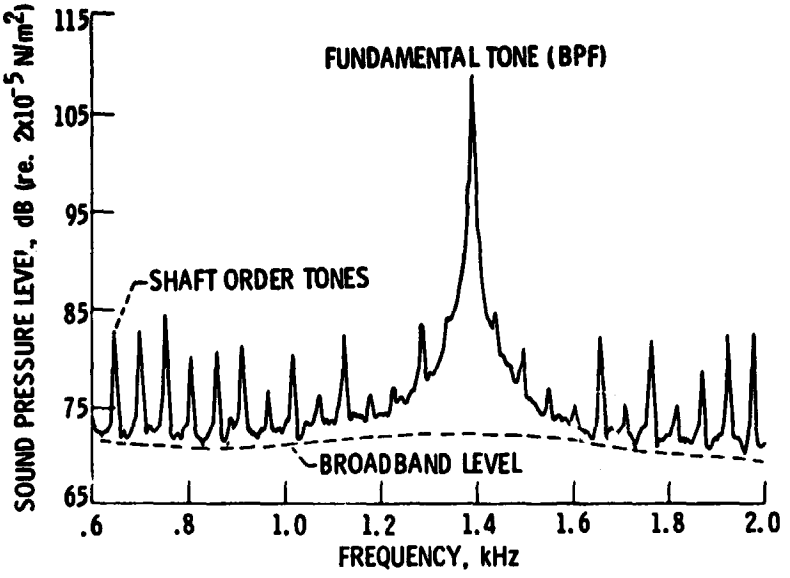

Figure 3. - Effect of random noise on fundamental tone narrow-band spectrum (fan B; 90 percent speed; 40° azimuth angle; 4 hertz bandwidth).

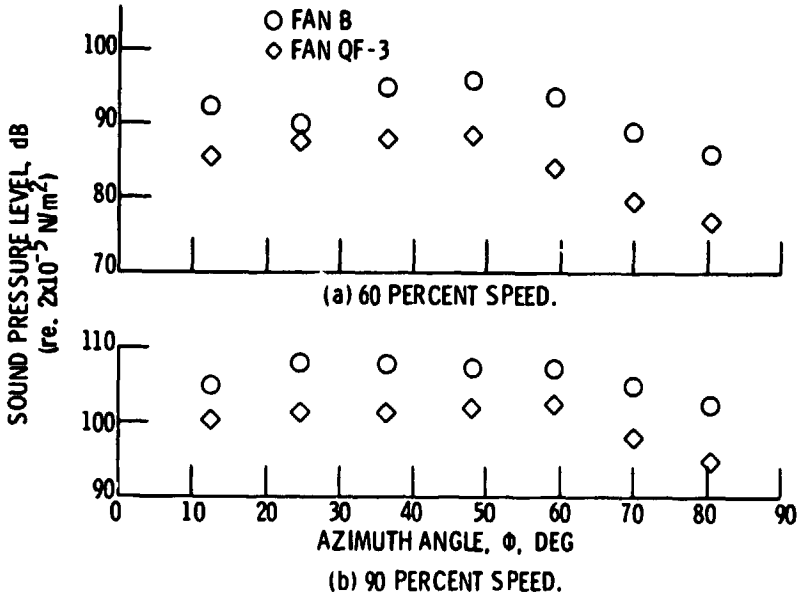

Figure 4. - Variation of sound pressure level of blade passing frequency tones of fans B and QF-3 with inlet angle.

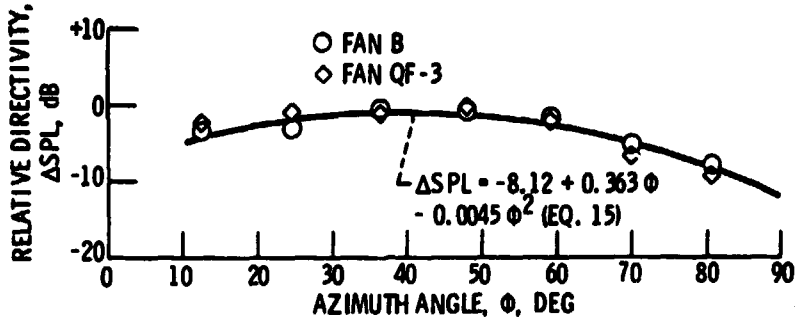

Figure 5. - Average normalized relative directivity of blade passing frequency tones of fans B and QF-3.

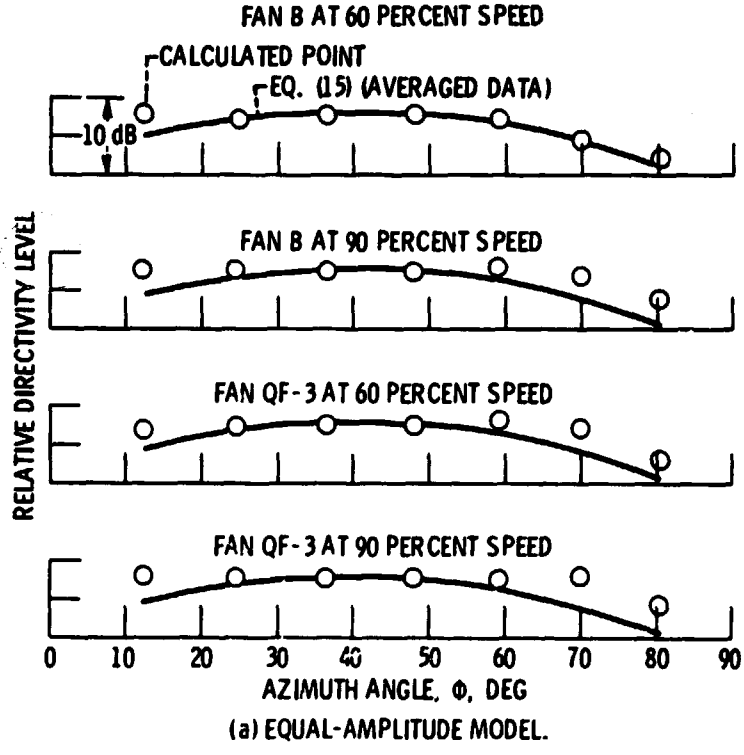

(a) EQUAL-AMPLITUDE MODEL.

Figure 6. - Comparison of theoretical and average experimental directivities.

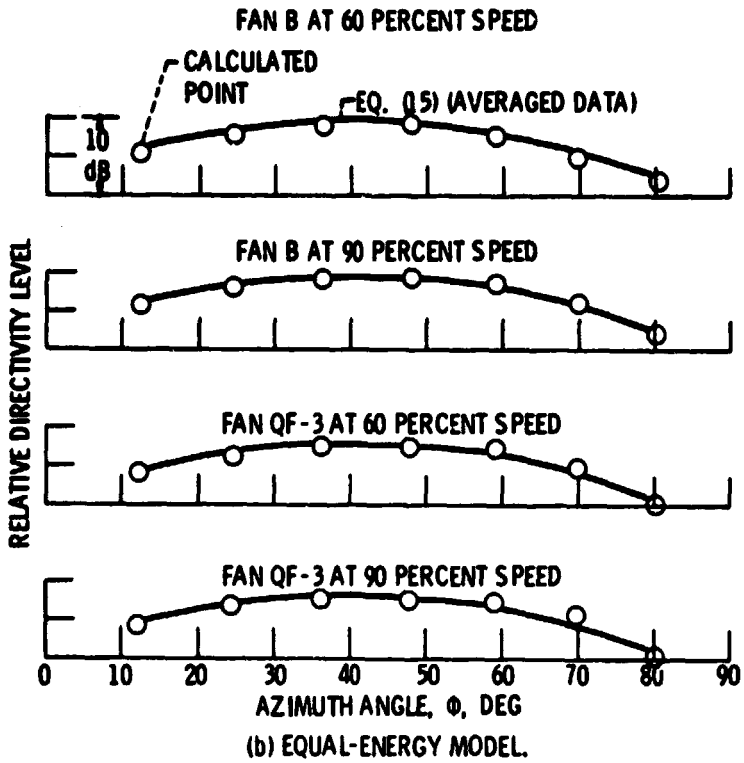

(b) EQUAL-ENERGY MODEL.

Figure 6. - Concluded.

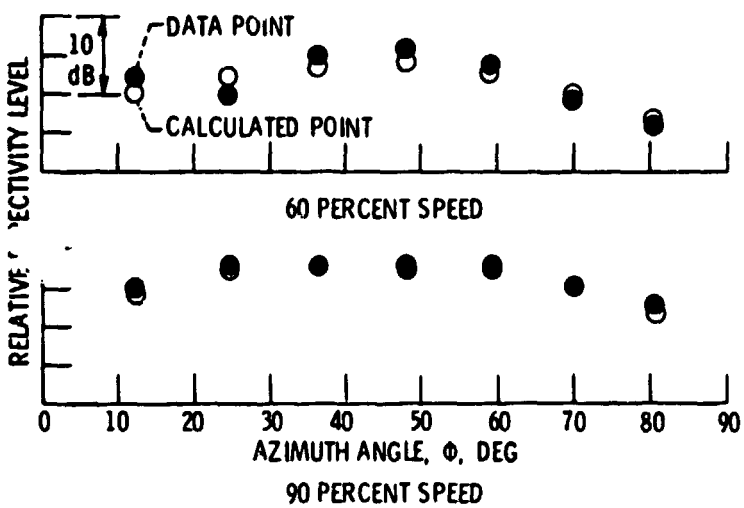

(a) FAN B.

Figure 7. - Comparison of theoretical (equal energy) and actual experimental directivities.

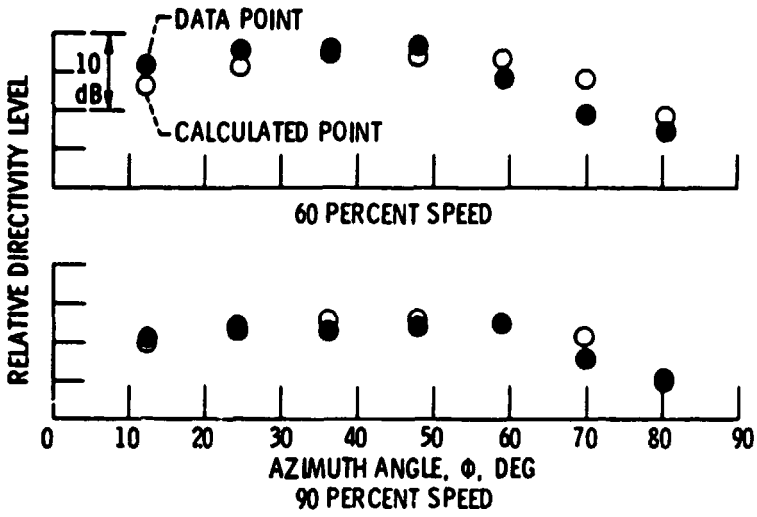

(b) QF-3 FAN.

Figure 7. - Concluded.